Iranian Journal of Medical Physics

ijmp.mums.ac.ir

Statistical Process Control in Monitoring Radiotherapy Quality Assurance Program: An Institutional Experience.

R. Vysakh[1,2*], R Ganapathi Raman[1], P. Niyas[2], P Aflah[2]

1. Department of Physics, Noorul Islam Centre for Higher Education, Kumaracoil- 629 180, Kanyakumari District, Tamilnadu, India.
2. Department of Medical Physics and Radiation Safety, MVR Cancer Centre & Research Institute, Calicut, India

ARTICLE INFO

Article type:
Original Paper

Article history:
Received: Feb 24, 2021
Accepted: Aug 29, 2021

Keywords:
Radiotherapy
Quality Assurance
Patient-Specific Quality Assurance
Statistical Process Control

ABSTRACT

Introduction: Statistical process control (SPC) is a handy and powerful tool for monitoring quality assurance (QA) programs in radiotherapy. This study explains the institutional experience in monitoring weekly output constancy QA and patient-specific quality assurance (PSQA) using SPC tools.

Material and Methods: Prospective monitoring of output constancy has been demonstrated by the simultaneous usage of Shewhart's I-MR charts and time-weighted control charts. PSQA results were retrospectively analysed in a combined γ and dose volume histogram (DVH) based analysis using control charts and process capability indices. A PSQA analysis method has been illustrated in which the site-specific action limits (AL) and control limits (CL) for γ and DVH based analysis were obtained using SPC.

Results: The simultaneous use of different control charts indicated a systematic error in the output constancy of Linac as successive measurement points fell above the CL. The reason for failure was found and process was monitored further. The obtained AL and CL for γ and DVH based analysis were used to decide pass or fail criteria in PSQA. Among the analysed treatment plans, fourteen plans of different treatment sites failed the PSQA analysis. Cause-and-effect analysis of these failed treatment plans in PSQA pointed out six primary potential sources of errors in the results.

Conclusion: SPC tools can be adopted among institutions for consistent and comparable QA programs. If the QA process monitored using SPC falls outside the CL, cause-and-effect diagrams can be used to extract all possible contributing factors that lead to such a process state.

►*Please cite this article as:*
Vysakh R, Ganapathi Raman R, Niyas P, Aflah P. Statistical Process Control in Monitoring Radiotherapy Quality Assurance Program: An Institutional Experience. Iran J Med Phys 2022; 19: 189-198. 10.22038/IJMP.2021.55869.1931.

Introduction

The advancement of technology in the last few decades of radiotherapy has made a tremendous impact on increasing treatment quality. The development has obliged each radiotherapy department to set up and perform dedicated quality assurance (QA) programs. These QA programs are mostly designed so that the measured system performance is compared with different international and national standard guidelines, and a conclusion is made. This 'goal post line' approach may often but not always reveal the real-time trend of the QA process in the radiotherapy department. Statistical process control (SPC) has emerged as a handy and powerful tool for monitoring QA processes in radiotherapy departments. SPC is efficient in monitoring the outcome of the QA process and ensures the quality of the observed QA result by pointing out systematic and random error components in the QA process [1]. This study explains the importance of using SPC methods in monitoring the rigorous QA processes of radiotherapy. This work can provide further information for using SPC tools and cause-and-effect diagrams for monitoring any QA process in radiotherapy.

Weekly output constancy is one of the necessary QA checks in radiotherapy, as any significant deviation in the machine's output results in a direct mismatch in the intended dose to the patient. The limits for this QA has been set using standard recommendations and guidelines [2]. Various authors [3-5] have demonstrated how SPC tools could be used for monitoring in output constancy of Linac.

The complexities associated with the VMAT in planning and treatment delivery has always demanded a pre-treatment PSQA. The proposed gamma analysis by Low et al. [6] is one of the widely accepted methods for the evaluation of PSQA. The introduction of new detectors and software tools in the PSQA programme offers more advanced dosimetric evaluation based on γ and dose volume histogram (DVH) based analysis of individual structures. Reviewing various studies on PSQA, American Association of Physicists in Medicine (AAPM) recently published their Task group report 218 (TG-218) [7], which recommends a dedicated PSQA with equipment specific and site-specific CL and AL derived based on SPC methods. They also suggested the usage of DVH based analysis of

*Corresponding Author: Tel: +91-8593825287; Email: vysakhraveendran92@gmail.com; ganapathiraman83@gmail.com

individual structures in the treatment plan to evaluate the clinical relevance of the QA results. Various authors have used SPC techniques to set AL and CL for PSQA [8, 9], but most of these works were either based on 2D γ measurement or point-dose measurements. In this work, AL and CL have separately obtained for 3D γ analysis and DVH based analysis, and a PSQA analysis combining these two is demonstrated.

Materials and Methods

Control charts

Quality characteristics of any sample or process can be represented by plotting the parameter under evaluation on the Y-axis and sample number or time on the X-axis; these two-dimensional representations are called control charts. The central line in a control chart represents the average value of the parameter under evaluation. Any QA process monitored using SPC will have action limits (AL) and control limits (CL) or tolerance limits. An AL defines a scale of allowable clinical results for a QA process such that any QA result outside the AL would demand urgent action by the physician to bring the process back within the criteria of acceptability. AL can be either defined locally using the local experience or derived from clinical evidence or consensus among global professional organisations or experts. CL refers to the scale within which the QA results are regarded as unvarying. The upper control limit (UCL) and lower control limit (LCL) act as warning limits or threshold limits for the parameter or process. A process is said to be 'in control' state when the values are within the boundaries set by UCL and LCL [10]. Four types of control charts were used for monitoring the different QA process in our department, which are Shewhart's individual value-moving range (I-MR) chart, exponentially weighted moving average chart (EWMA chart), and cumulative sum (CUSUM) charts. Control charts were introduced in analysing output constancy results at our department from 2018 onwards. QA results were analyzed by a single physicist or resident physicists under the supervision of a senior physicist using different control charts. After an initial retrospective analysis of last year's output constancy results, the parameters associated with each control chart were finalised. The prospective analysis of output constancy results was then started using these control charts. Most control charts favour data monitoring when the data is normally distributed; we have checked the normality of the data distribution by the Anderson-Darling test for normality. All control charts and statistical analysis shown in this study were drawn in Minitab® 18.1 version.

Shewhart's individual value chart (I-Chart) and moving range (MR) chart

Individual QA results are plotted against the measurement number in an I-chart, while differences between consecutive QA results (range) are used in the MR chart. An I-MR chart is useful in detecting large shifts in processes (≥1.5 standard deviation, σ) and those processes in which data are added slowly so that subgrouping data is difficult for drawing control charts [10]. Parameters for an I-chart are defined as follows:

$$UCL = \bar{x} + 3\frac{\overline{MR}}{d_2} \quad (1)$$

$$Center\ line = \bar{x} \quad (2)$$

$$LCL = \bar{x} - 3\frac{\overline{MR}}{d_2} \quad (3)$$

Similarly, for an MR chart

$$UCL = (1 + 3\frac{d_2}{d_3})\,\overline{MR} \quad (4)$$

$$Center\ line = \overline{MR} \quad (5)$$

$$LCL = (1 - 3\frac{d_2}{d_3})\,\overline{MR} \quad (6)$$

Where $\bar{x}$ and $\overline{MR}$ represents process average and average moving range used to define the CL in the monitored QA process, respectively. d_2 and d_3 are constants, and in this study, their values are 1.128 and 0.8525, respectively [10].

The cumulative sum (CUSUM) control chart.

A CUSUM chart is generated by plotting cumulative sums of the variation of the sample values from a set target value versus sample number [10]. Cumulative sum up to and including the *i*th sample is given by

$$C_i = \sum_{j=1}^{i}(x_j - T) \quad (7)$$

x_j is the sample value and T is the target value. C_i will move around zero if the process is under control ($x_j = T$), or it will signal if the process drifts away from T. These drifts can be expressed via one-sided upper (C_i^+ ($x_j > T$)) or lower (C_i^- ($x_j < T$)) tabular CUSUM. Tabular CUSUM indicates the direction of shifting of sample/process parameters under evaluation, and these are calculated as follows:

$$C_i^+ = \max\,[0, x_i - (T + K) + C_{I-1}^+] \quad (8)$$

$$C_i^- = \max\,[0, x_i - (T + K) + C_{I-1}^-] \quad (9)$$

When $i = 0$, C_i^-, $C_i^+ = 0$. K is the reference value or the allowance value. One can choose the value of K depending upon the magnitude of shifts that needed to be monitored using a CUSUM chart.

$$K = \frac{\Delta}{2}\sigma \quad (10)$$

where the term $\Delta\sigma$ is the smallest shift to be detected, expressed in terms of standard deviation. For monitoring output constancy using CUSUM control charts, K is chosen as 0.5 and the decision interval (H) as 5[10].

Exponentially weighted moving average (EWMA) control chart

An EWMA chart can be used to find small drift in the QA process because of its peculiar construction. Every point in an EWMA chart is derived from weighted averages of the past, with the highest weight being given to recent data point and then the degree of weight decreases exponentially based on the chronological proximity to the present data point [10]. The EWMA value z_i, of x_i th data point, is defined mathematically as

$$z_i = \lambda x_i + (1-\lambda) z_{i-1} \quad (11)$$

Where z_{i-1} is the EWMA value of the x_{i-1} th data point and λ $(0 < \lambda \leq 1)$ is the constant that decides the weight of prior data points via exponential function λ $(1-\lambda)$, λ $(1-\lambda)^2$, etc. The first EWMA value is the process target, $z_0 = T$. The CL for an EWMA chart is calculated using the following equations.

$$UCL = \mu_0 + L\sigma\sqrt{\frac{\lambda}{(2-\lambda)}\left[1-(1-\lambda)^{2i}\right]} \quad (12)$$

$$Central\ line = \mu_0 \quad (13)$$

$$LCL = \mu_0 - L\sigma\sqrt{\frac{\lambda}{(2-\lambda)}\left[1-(1-\lambda)^{2i}\right]} \quad (14)$$

Where μ_0 is the process average, and the factor L decides the width of CL. For monitoring output constancy, L and λ were chosen as 3 and 0.2, respectively [10].

Process capability indices (PCI).

Process capability indices are used to estimate the variability of a process over time within its tolerance limits and understand how centered the process is about the target value. Before using PCI, the process must remain in a state of statistical control. Generally, for ensuring statistical stability, control charts are used and the process is monitored until it reaches statistical stability. C_p and C_{pk} are two commonly used PCI in quality management [10]. A two-sided C_{pm} index for normal data is calculated as follows

$$C_{pm} = \frac{UAL-LAL}{A\sqrt{\sigma^2+(\bar{x}-T)}} \quad (15)$$

Where A is the constant that describes the level quality of needed, σ and $\bar{x}$ are the process standard deviation and process mean. A C_{pm} value of 1.33 is typically used for an acceptably performing process [10].

Cause-and-effect diagram

It is always challenging for physicists to analyze and find potential reasons once the monitored QA process loses its state of statistical control. In these scenarios where the reasons are not clear, the cause-and-effect diagram or the fishbone diagram can be used to extract all possible contributing factors that lead to such a process state [10]. A cause-and-effect diagram created in an ordered manner can be utilised to find the causes for QA failure and further corrective actions can be taken. In the present work, a team of five physicists and a service engineer was formed for cause-and-effect analysis of output constancy results, while a team of four physicists was assigned for cause-and-effect analysis of PSQA.

Weekly output constancy QA

Output constancy test of Elekta Synergy Linac (Elekta, Stockholm, Sweden) was performed in solid water equivalent phantoms using farmer type (FC-65) ion chamber and Dose-1 Electrometer (IBA Dosimetry, Schwarzenbruck, Germany). The QA consists of measuring the charge collected for 200 monitor units (MUs) for 10 × 10 cm^2 radiation field at 5 cm depth in solid water phantom. The correction factor for air temperature and air pressure (k_{tp}) was also applied to the chamber readings. For weekly output constancy, the baseline readings were taken once the machine output was tuned as per the Technical Report Series No.398 (TRS-398) protocol [11], and these results were compared to the baseline readings.

Patient-specific QA (PSQA) using Dolphin detector and Compass dosimetry:

Treatment plans were generated on the Monaco treatment planning system (TPS) ver. 5.11 (Elekta, Stockholm, Sweden), and PSQA was performed using Dolphin detector™ and Compass dosimetry system™ from IBA Dosimetry (Schwarzenbruck, Germany). Measurements were performed in Linacs, VersaHD and Synergy (Elekta, Stockholm, Sweden). The Dolphin detector comprises a pixel segmented ion chamber, i.e., a 2D detector array consisting of 1513 air-vented parallel plate ion chambers with a total active measurement area of 24 × 24 cm^2 [12]. In the study for PSQA, the Reference dose distribution (Rdd) was compared with the TPS dose distribution (TPSdd) using both 3D γ and DVH based evaluation as recommended by AAPM TG-218 [7]. Parameters for 3D γ analysis consist of global dose normalisation to the highest prescription dose in the treatment plan, 10 % dose threshold to exclude insignificant dose levels, γ criteria of 2 mm distance to agreement (DTA) and 3 % dose difference. For DVH based dose evaluation, the percentage difference (% DD) in the dose received by the 95% planning target volume (PTV) was calculated as follows,

$$\%\,DD = \left|\frac{D95_{TPSdd} - D95_{Rdd}}{D95_{TPSdd}}\right| \times 100 \quad (16)$$

where $D95_{TPSdd}$ is the dose received by 95% volume of PTV in the TPSdd and $D95_{Rdd}$ is the dose received by 95% volume of the PTV in the Rdd. Table 1 represents the site-specific list of VMAT plans in which PSQA measurements are performed.

Table: Site-specific number of VMAT plans	Head and neck (HN)	Central nervous system (CNS)	Gastro intestinal (GI) and Gastro urology (GU)	Lung	Stereotactic body radiotherapy (SBRT)
No. of cases	104	41	46	23	27

Setting site-specific action limits and control limits for PSQA using SPC

PSQA analysis consists of a combination of both 3D γ and DVH analysis. For 3D γ analysis, the percentage γ pass rate for structures patient (patient %GP) and PTV (PTV %GP) were used, while for DVH analysis % DD for PTV D95 was considered. Shewhart's I-MR chart was used to monitor the PSQA results and CL was obtained separately for 3D γ analysis and DVH analysis. In this study, the initial 20 PSQA results were used to obtain the CL for each site. Once the PSQA result was within the CL, the AL was calculated by rearranging equations for process capability indices (equation 15).

$$\Delta AL = \beta\sqrt{\sigma^2 + (\bar{x} - T)^2} \quad (17)$$

Where ΔAL is the width of action limits, commonly written as $\pm AL/2$, σ and $\bar{x}$ is the standard deviation and mean of the chosen PSQA results. T is the target value to be achieved; generally, in the 3D γ analysis this value is chosen as 100 %, and for DVH based analysis it is chosen as 0 %. In finding AL for γ analysis and DVH analysis, β is chosen as 6 [13]. The clinical feasibility of the obtained AL for DVH analysis was discussed with the radiation oncologist before finalising. If the obtained AL for DVH analysis was not clinically feasible, the value for β in equation 18 was modified. Based on the literature [14], 2D plots were created between PTV %GP and %DD in PTV D95 on a site-specific basis. The obtained AL was used to divide the plot into four distinct regions (True negatives, True positives, False negatives and False positives), as shown in figure 1.

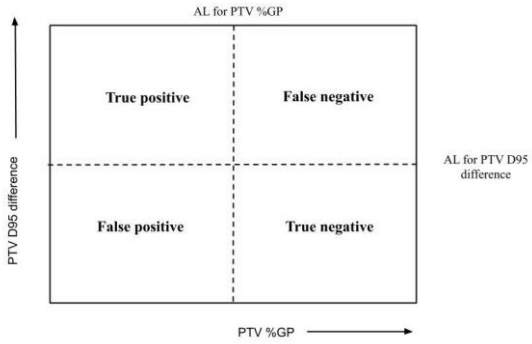

Figure 1. 2D plot used for combined γ and DVH based analysis of the PTV.

PSQA plans were analysed in detail, depending upon in which region the QA results fall in these 2D plots. A treatment plan is considered as failed if the patient %GP is exceeding the AL or if the PSQA result falls in the true positive region of the 2D plot. If the patient %GP is below AL and the QA result falls either in the false negative or false positive region, an objective assessment of the QA plan is required considering the clinical feasibility.

Results

Prospective SPC analysis of output constancy.

Control charts used for monitoring output constancy

The results of 69 output constancy QA measurements for June 2019 to March 2020 for three different photon energies are presented using control charts in figures 2-4. Each control chart has two distinct stages, in which stage-1 consists of 50 output constancy QA results and stage-2 contains 19. Stage-1 shows the QA results with a systematic error within the process, while stage-2 shows the QA results after removing this uncertainty. Each control chart has its own CL obtained using the initial ten readings. For an I-chart in addition to the CL universal AL (± 3 %) [2] of the output constancy are also plotted as dashed lines.

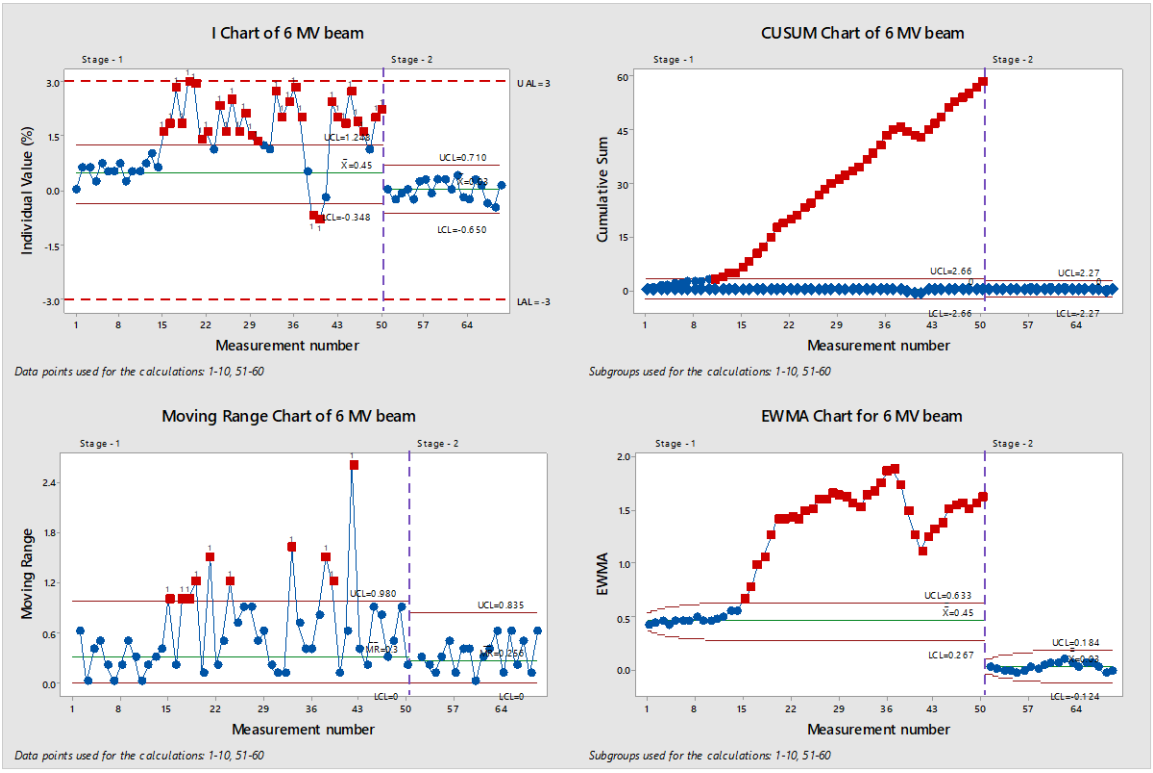

Figure 2. Control charts for output constancy of 6 MV beam

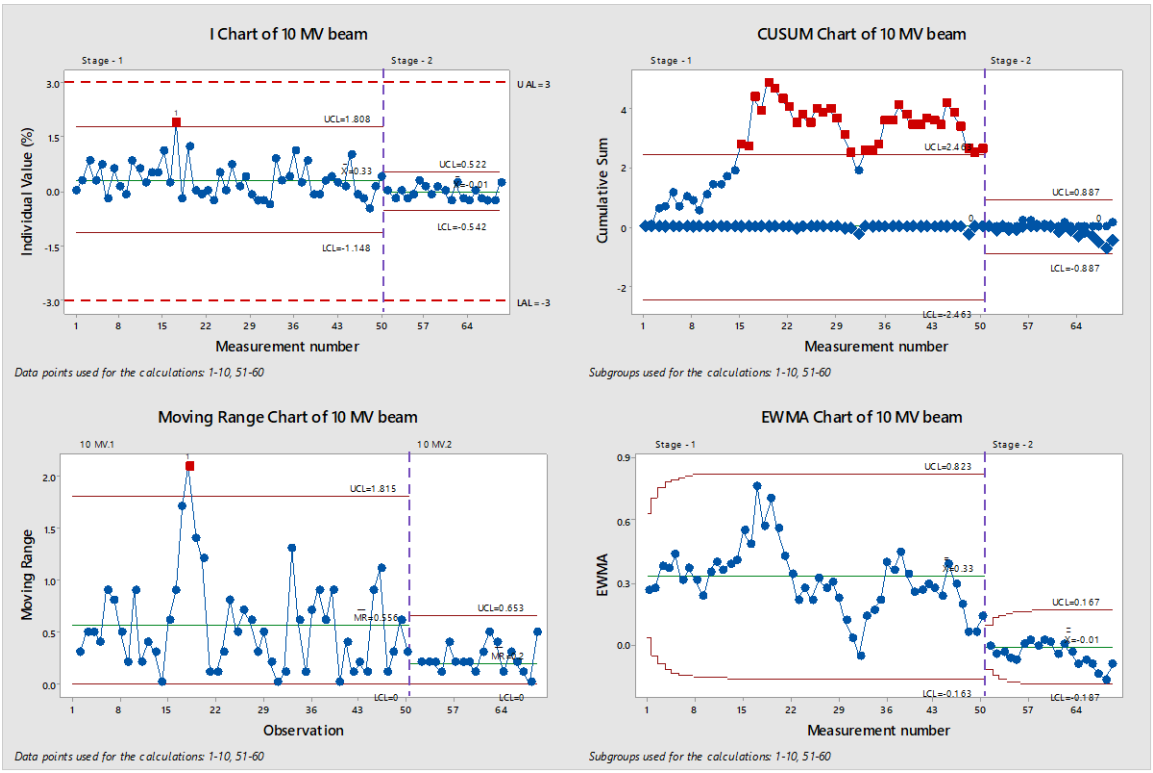

Figure 3. Control charts for output constancy of 10 MV beam

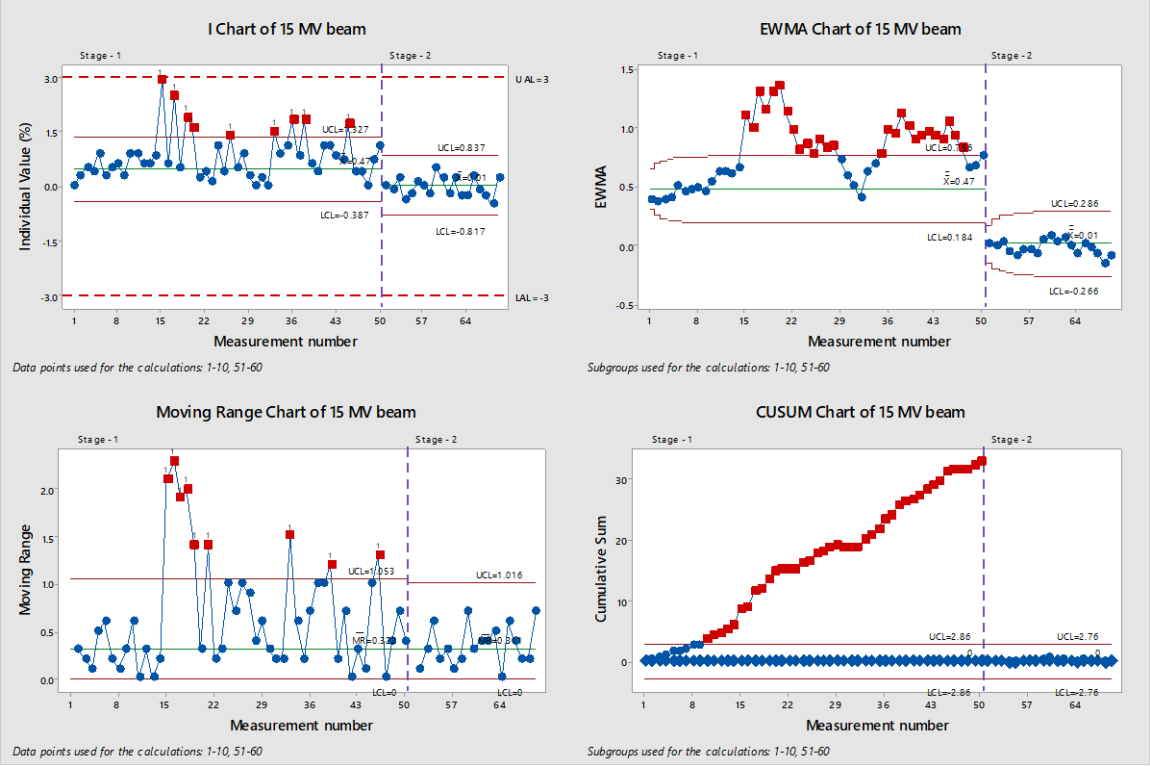

Figure 4. Control charts for output constancy of 15 MV beam

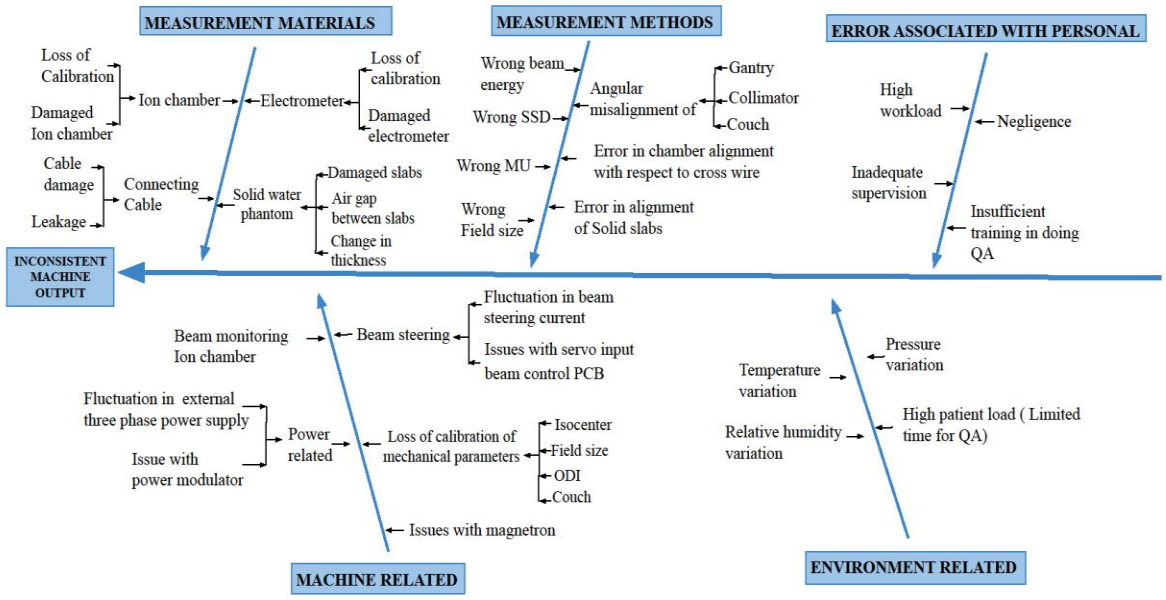

Figure 5. Cause-and-effect diagram used for analysing output constancy of Linac.

Cause-and-effect diagram for output constancy monitoring

The possible reasons for a variation in output constancy results were listed via brainstorming and a cause-and-effect diagram was plotted, as shown in figure 5. The five major branches of the plot were broken down into different sub-branches by adding each element that would contribute to an error in the output constancy results. Each component of the plots was examined one by one and a thorough root cause analysis was done using this plot.

Retrospective SPC analysis of site-wise PSQA results.

Control charts and 2D plots

The 2D plots obtained from PSQA analysis for each site are shown in figure 6 and the associated control charts are given in supplementary material. Table 2 compares the CL and AL obtained using the initial 20 PSQA for different sites. For the Head and neck (HN) site, ten plans exceeded the patient %GP action limit; two out of ten were true positive. Six HN plans with %GP above CL but within the AL were false positive. Detailed PTV γ analysis of these false-positive plans showed that the γ failures were at the edges of the PTV for four plans and were

near the tumor for the other two plans. Thus, those four plans were considered passed, and the other two failed PSQA. Five HN true negative plans had patient %GP above the CL, but within the AL, major γ failures were near the normal tissues such as the parotid and larynx, where there was a steep dose gradient. These plans were considered passed PSQA based on discussion with the radiation oncologist. Only two Central nervous system (CNS) plans failed PSQA as their patient %GP was greater than the AL. These failed cases were false positives, and the rest of all passed cases were true negatives. More considerable inhomogeneities associated with lung plans have increased AL for patient %GP, PTV %GP and % DD in PTV D95. Three Gastro-Intestinal (GI) and Gastro Urology (GU) plans had patient %GP above AL in which two were true positive, and one was false positive. These three cases and two additional true positive cases were considered as failed the PSQA due to significant γ failures inside PTV and at organs at risk. Compared to other sites, Stereotactic body radiotherapy (SBRT) plans have a larger patient %GP with the central line, LCL and LAL at 99.17%, 97.54%, and 96.86%, respectively. However, these plans showed lower PTV %GP and larger %DD in PTV D95 than other conventional VMAT plans.

Cause-and-effect diagram for analysis PSQA results

Figure 7 shows the cause-and-effect diagram used for the root cause analysis of the failed PSQA. Six significant reasons for PSQA failures were identified, and these were divided into sub-branches.

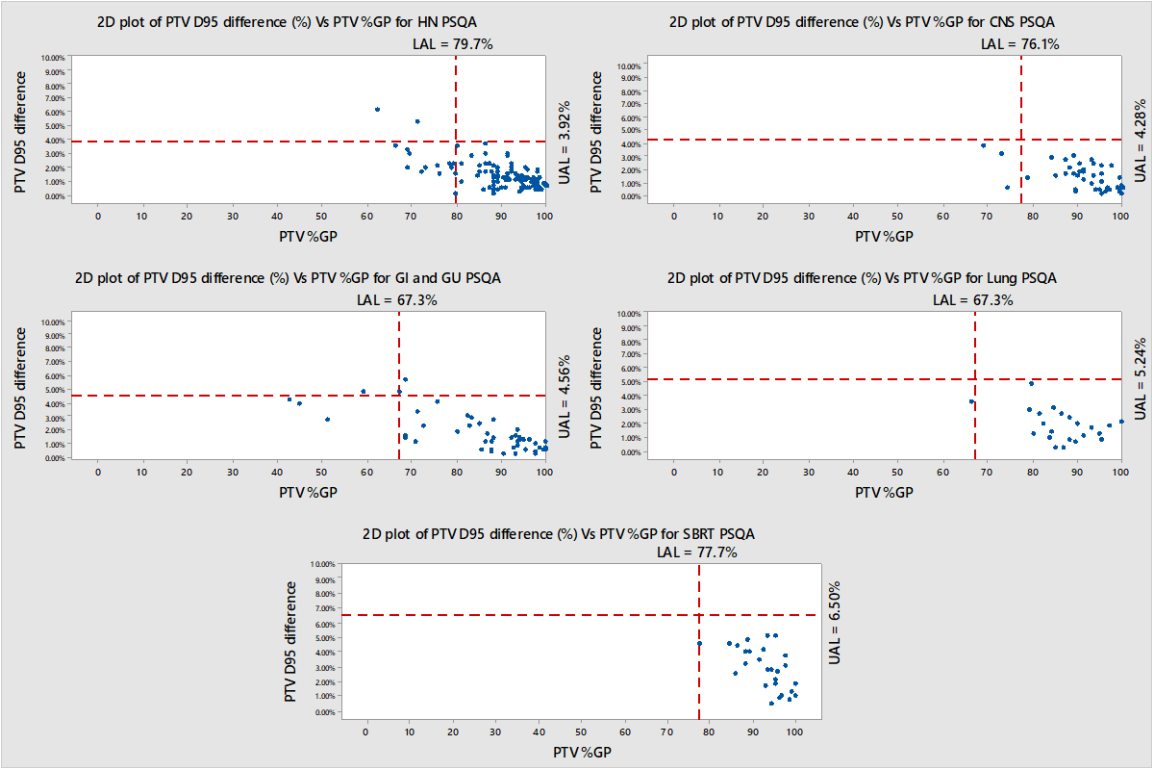

Figure 6. Site-wise 2D plots of the PSQA results

Table 1. Site-specific CL and AL obtained using the initial 20 PSQA results

Site	Structure and criteria for evaluation	Control limits obtained from I-chart			Action limits	
		Central line (%)	LCL (%)	UCL (%)	LAL (%)	UAL (%)
HN	Patient %GP	96.94	93.29	-	90.1	-
	PTV %GP	94.23	85.11	-	79.7	-
	%DD in PTV D95	1.17	-	3.11	-	3.92
CNS	Patient %GP	97.52	92.87	-	91.31	-
	PTV %GP	93.17	80.13	-	76.1	-
	%DD in PTV D95	1.15	-	3.31	-	4.28
Lung	Patient %GP	95.23	88.66	-	87	-
	PTV %GP	88.24	71.42	-	67.3	-
	%DD in PTV D95	1.52	-	4.93	-	5.24
GI and GU	Patient %GP	96.67	89.61	-	88	-
	PTV %GP	90.93	72.77	-	67.27	
	%DD in PTV D95	1.21	-	3.77	-	4.65
SBRT	Patient %GP	99.17	97.54	-	96.86	-
	PTV %GP	93.78	85.12		77.67	
	%DD in PTV D95	2.38		5.15		6.4

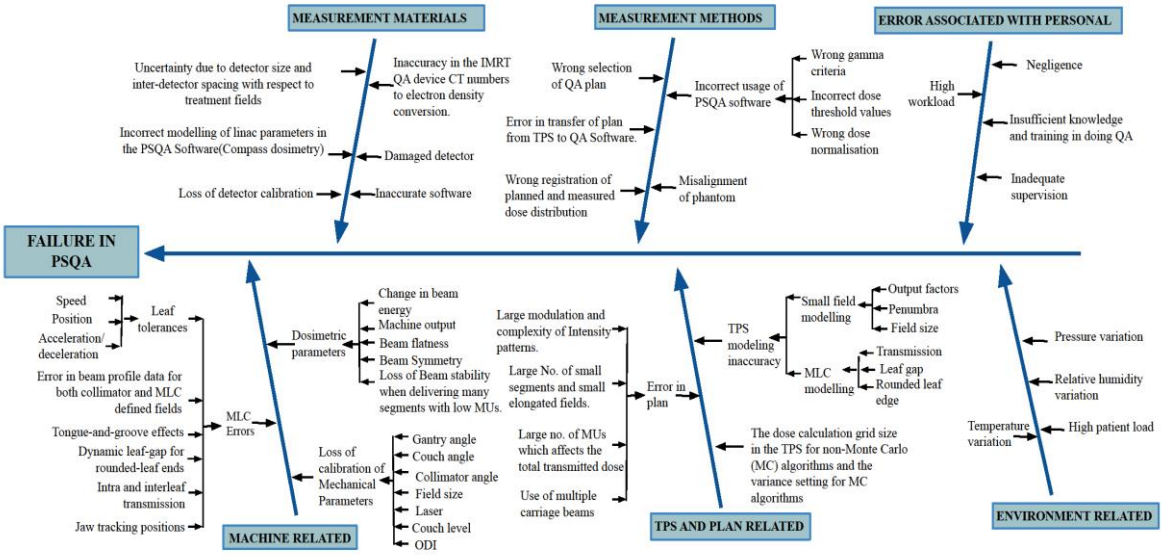

Figure 7. Cause-and-effect diagram for analysing PSQA.

Discussion

Prospective SPC analysis of output constancy

The simultaneous use of four control charts for prospective monitoring output constancy results of Linac successfully demonstrated the real-time QA trend. In stage-1, the CUSUM charts of 6 MV and 15 MV photon beams showed a slow drift in the process because the 12th measurement data went outside the CL. Since the process was under the CL in the other three control charts, it was decided to continue to monitor the process further. A noticeable drift was observed at the 15th measurement point, where the data of 6 MV and 15 MV beams deviated from CL in the other three control charts. Also, in the I-chart of 15 MV beam, the 15th measurement point showed a variation of +2.9%, which was almost as high as the UAL. An error was suspected within the process; another team of physicists under the supervision of a senior physicist repeated the measurements with the same apparatus on the same day. This result is shown as the 16th measurement point in the control charts, which shows a lesser variation in readings except for 6 MV. Thus, the reproducibility and accuracy of the measurement apparatus were suspected. However, the output constancy of Versa Linac measured with the same apparatus was consistent. Hence absolute calibration of Synergy Linac was performed on the same day with standard reference conditions as per the TRS-398 protocol [11]. The maximum variation in the machine's output was only 0.67 % for 6 MV beam. The issue was discussed with the service engineer, and decided to repeat the measurements daily before and after patient treatment on both machines with the same apparatus. The stage -1 measurement points 17 to 50 in the control chart shows these results measured before and after patient treatment. Even if the measurement points were above CL, none of them went above the AL in the I-chart for any photon energy; hence the patient treatment was not interrupted. Meanwhile, four physicists and a service engineer formed a team to monitor the output constancy QA process and do a cause-and-effect analysis.

The variation for the 10 MV beam was less than the other two beam energies; however, the CUSUM charts could find a drift for this beam. This is due to the peculiar construction of the CUSUM chart, which is more sensitive to get a drift in the order of 1σ. However, a consistent output constancy QA result of 1% would be indicated as an out-of-control process in the CUSUM if the CUSUM target is 0%. A combined CUSUM-Shewhart procedure can be used to monitor the QA process for detecting massive shifts, while time-weighted control charts alone can detect slight drift in the process of the order of 1 sigma [10].A root cause analysis based on a cause-and-effect diagram has helped analyse each component suspected of an unstable output deviation. The possibility of an error due to the measurement system was ruled out as the output constancy results of the Versa Linac, measured by using the same apparatus, were consistent with their previous values. The repeated measurement by another team of physicists under a senior physicist's supervision helped rule out the possible chance of errors due to measurement methods and personals. Environmental factors such as relative humidity and temperature can affect the Linac output [15]. Relative humidity and temperature recorded using a calibrated Humidity-temperature data logger inside the treatment room ensured no significant fluctuation in the relative humidity and temperature values. There was no significant improvement in the output constancy results after checking factors related to power fluctuation and beam steering; the monitor ion chamber's working was evaluated in detail. Various authors have reported a shift in the Linac output due to faulty monitor chambers [16,

17]. Detailed analyses conclude that the unsealed monitor chamber of the Linac was found faulty. This monitor chamber was changed and beam parameters were tuned to match the original values. New baseline readings were taken for output constancy check and the process monitoring was continued using control charts. These results are shown as stage-2 in the control charts (figure 2 to figure 4), in which new CL was obtained to monitor the process further.

Retrospective SPC analysis of site-wise PSQA results

Monitoring PSQA using control charts enables continuous enhanced process monitoring. The presence of variation due to readily assignable causes and variation due to non-readily assignable causes can be separated [1]. Cause-and-effect analysis pointed out different assignable causes to those cases which failed PSQA measurements. Two of these were due to the wrong registration of the planned and measured dose distribution, while in four false-positive plans, wrong dose normalisations were selected for γ analysis. The increased γ failures near and inside PTVs in SBRT, can be due to extensive plan modulation, the complexity of small field intensity patterns, and the uncertainty of the Dolphin detector. The Prostate plans made according to the CHHiP trials [18] demands higher plan modulations for attaining the required dose constraints. The PSQA results of these plans exhibited γ failures in the areas where the PTV overlapped with the rectum and bladder, which caused elevated CL and AL in the GI and GU sites. The VMAT plans for whole-brain radiotherapy with hippocampus sparing, failed PSQA measurements because of complex plan modulation and large numbers of small segments; the failed CNS PSQA measurements

Various authors have reported the CL and AL for γ analysis in PSQA using SPC [8-9]. Sanghangthum et al. [8] found patient %GP (3 %/ 3mm γ criteria at 10 % dose threshold) LCL as 85 % for HN Intensity modulated radiotherapy (IMRT) and 90.3 % for HN VMAT plans. Rena Lee et.al [9] reported patient %GP (3%/3mm γ criteria) LCL as 98.8 %, 98.1 %, 85.4 % for HN, Prostate and Breast plans, respectively. Since the above limits were obtained with different γ criteria and with a different detector system, a direct comparison of these results with the present study's obtained limits would result in improper conclusions. TG -218 recommends LCL and LAL for patient %GP (3%, 2mm γ criteria at 10% dose threshold) as 95 % and 90 %, respectively. The obtained LCL and AL for patient %GP in this study were comparable to these recommended limits except for Lung, GI and GU sites. There have been various reports and studies [19-20] related to the AL of DVH analysis in PSQA, suggesting an AL of 5% for the DVH-based analysis. The UAL obtained for DVH analysis using SPC in this study was comparable to the suggested limit of 5%. The maximum value for UAL was obtained for SBRT plans as 6.4 %. The TG-218 also recommends for γ analysis on a structure-by-structure basis incorporating the DVH analysis. This study demonstrates this method of analysis for PTV in VMAT plans, which adds more clinical relevance to PSQA. As a future perspective, finding AL and LCL for γ analysis and DVH analysis for targets as well as for normal structures on a site-wise/ technique basis will provide more insights into PSQA.

Conclusion

This study demonstrates the institutional experience in monitoring two different radiotherapy QA processes using SPC. The simultaneous use of Shewhart's control charts and time-weighted control charts successfully exhibited the real-time trend of output constancy of Linac. The cause-and-effect analysis of the study leads to find the faulty monitor chamber of the Linac as the source for systematic error in the weekly QA process. A PSQA analysis method was introduced in which the AL and CL for γ and DVH-based comparisons were obtained via SPC. Cause-and-effect analysis of the plans that failed in PSQA pointed out potential sources of errors in the PSQA program.

Acknowledgment

The authors are grateful to Elekta service engineer Mr. Syam Mohan for his advice and invaluable help with the Linac maintenance. The authors would also like to thank Dr. Narayanan Kutty Warrier, Medical Director, MVR Cancer Centre and Research Institute for permitting the facilities for conducting the experiments.

References

1. Pawlicki T, Whitaker M, Boyer AL. Statistical process control for radiotherapy quality assurance. Medical physics. 2005;32(9):2777-86.
2. Klein EE, Hanley J, Bayouth J, Yin FF, Simon W, Dresser S, et al. Task group 142 report: quality assurance of medical accelerators. Med Phys. 2009;36(9):4197–212.
3. Sanghangthum T, Suriyapee S, Srisatit S, Pawlicki T. Retrospective analysis of linear accelerator output constancy checks using process control techniques. Journal of applied clinical medical physics. 2013;14(1):147-60.
4. Binny D, Mezzenga E, Lancaster CM, Trapp JV, Kairn T, Crowe SB. Investigating output and energy variations and their relationship to delivery QA results using Statistical Process Control for helical tomotherapy. Physica Medica. 20171;38:105-10.
5. Pal B, Pal A, Das S, Palit S, Sarkar P, Mondal S, et al. Retrospective study on performance of constancy check device in Linac beam monitoring using Statistical Process Control. Reports of Practical Oncology & Radiotherapy. 2020;25(1):91-9.
6. Low DA, Harms WB, Mutic S, Purdy JA. A technique for the quantitative evaluation of dose distributions. Medical physics. 1998;25(5):656-61.
7. Miften M, Olch A, Mihailidis D, Moran J, Pawlicki T, Molineu A, et al. Tolerance limits and methodologies for IMRT measurement-based verification QA: recommendations of AAPM Task Group No. 218. Medical physics. 2018;45(4):e53-83.
8. Sanghangthum T, Suriyapee S, Srisatit S, Pawlicki T. Statistical process control analysis for patient-

specific IMRT and VMAT QA. Journal of radiation research. 2013;54(3):546-52.
9. Lee R, Kim K, Cho S, Lim S, Lee S, Shim JB, et al. Statistical process control analysis for patient quality assurance of intensity modulated radiation therapy. Journal of the Korean Physical Society. 2017;71(10):717-21.
10. Montgomery DC. Introduction to statistical quality control. Hoboken, New Jersey:John Wiley & Sons,Inc.; 2009.
11. International Atomic Energy Agency. Absorbed dose determination in external beam radiotherapy: an international code of practice for dosimetry based on standards of absorbed dose to water, IAEA TRS-398. Vienna, Austria: IAEA, 2001.
12. Puzhakkal N, Kochunny AK, Makuny D, MP AK, Poyil RC, Raveendran V. Validation of Dolphin dosimetry in a three dimensional patient-specific quality assurance programme. Reports of Practical Oncology & Radiotherapy. 2019;24(5):481-90.
13. Sanghangthum T, Suriyapee S, Kim GY, Pawlicki T. A method of setting limits for the purpose of quality assurance. Physics in Medicine & Biology. 2013;58(19):7025.
14. Yi X, Lu WL, Dang J, Huang W, Cui HX, Wu WC, et al. A comprehensive and clinical-oriented evaluation criteria based on DVH information and gamma passing rates analysis for IMRT plan 3D verification. Journal of Applied Clinical Medical Physics. 2020;21(8):47-55.
15. Bartolac S, Heaton R, Norrlinger B, Letourneau D. Seasonal variations in measurements of linear accelerator output. Journal of applied clinical medical physics. 2019;20(3):81-8.
16. Grattan MW, Hounsell AR. Analysis of output trends from Varian 2100C/D and 600C/D accelerators. Physics in Medicine & Biology. 2010;56(1):N11.
17. Chan MF, Li Q, Tang X, Li X, Li J, Tang G, Hunt MA, Deasy JO. Visual analysis of the daily QA results of photon and electron beams of a trilogy Linac over a five-year period. Int J Med Phys Clin Eng Radiat Oncol. 2015;4(4):290-9
18. Dearnaley D, Syndikus I, Mossop H, Khoo V, Birtle A, Bloomfield D, et al. Conventional versus hypofractionated high-dose intensity-modulated radiotherapy for prostate cancer: 5-year outcomes of the randomised, non-inferiority, phase 3 CHHiP trial. The Lancet Oncology. 2016;17(8):1047-60.
19. Alber M, Broggi C, De Wagter C et al Guidelines for the verification of IMRT. ESTRO booklet. 2008.
20. Yi J, Han C, Zheng X, Zhou Y, Deng Z, Xie C, et al. Individual volume-based 3D gamma indices for pre-treatment VMAT QA. Journal of Applied Clinical Medical Physics. 2017;18(3):28-36.